

# Nuclear Effects on Hadron Production in d+Au and p+p Collisions at $\sqrt{s_{NN}}=200$ GeV

S.S. Adler,<sup>5</sup> S. Afanasiev,<sup>20</sup> C. Aidala,<sup>10</sup> N.N. Ajitanand,<sup>44</sup> Y. Akiba,<sup>21,40</sup> A. Al-Jamel,<sup>35</sup> J. Alexander,<sup>44</sup> K. Aoki,<sup>25</sup> L. Aphecetche,<sup>46</sup> R. Armendariz,<sup>35</sup> S.H. Aronson,<sup>5</sup> R. Averbek,<sup>45</sup> T.C. Awes,<sup>36</sup> V. Babintsev,<sup>17</sup> A. Baldisseri,<sup>11</sup> K.N. Barish,<sup>6</sup> P.D. Barnes,<sup>28</sup> B. Bassalleck,<sup>34</sup> S. Bathe,<sup>6,31</sup> S. Batsouli,<sup>10</sup> V. Baublis,<sup>39</sup> F. Bauer,<sup>6</sup> A. Bazilevsky,<sup>5,41</sup> S. Belikov,<sup>19,17</sup> M.T. Bjornndal,<sup>10</sup> J.G. Boissevain,<sup>28</sup> H. Borel,<sup>11</sup> M.L. Brooks,<sup>28</sup> D.S. Brown,<sup>35</sup> N. Bruner,<sup>34</sup> D. Bucher,<sup>31</sup> H. Buesching,<sup>5,31</sup> V. Bumazhnov,<sup>17</sup> G. Bunce,<sup>5,41</sup> J.M. Burward-Hoy,<sup>28,27</sup> S. Butsyk,<sup>45</sup> X. Camard,<sup>46</sup> P. Chand,<sup>4</sup> W.C. Chang,<sup>2</sup> S. Chernichenko,<sup>17</sup> C.Y. Chi,<sup>10</sup> J. Chiba,<sup>21</sup> M. Chiu,<sup>10</sup> I.J. Choi,<sup>53</sup> R.K. Choudhury,<sup>4</sup> T. Chujo,<sup>5</sup> V. Cianciolo,<sup>36</sup> Y. Cobigo,<sup>11</sup> B.A. Cole,<sup>10</sup> M.P. Comets,<sup>37</sup> P. Constantin,<sup>19</sup> M. Csanád,<sup>13</sup> T. Csörgő,<sup>22</sup> J.P. Cussonneau,<sup>46</sup> D. d'Enterria,<sup>10</sup> K. Das,<sup>14</sup> G. David,<sup>5</sup> F. Deák,<sup>13</sup> H. Delagrangé,<sup>46</sup> A. Denisov,<sup>17</sup> A. Deshpande,<sup>41</sup> E.J. Desmond,<sup>5</sup> A. Devismes,<sup>45</sup> O. Dietzsch,<sup>42</sup> J.L. Drachenberg,<sup>1</sup> O. Drapier,<sup>26</sup> A. Drees,<sup>45</sup> A. Durum,<sup>17</sup> D. Dutta,<sup>4</sup> V. Dzhordzhadze,<sup>47</sup> Y.V. Efremenko,<sup>36</sup> H. En'yo,<sup>40,41</sup> B. Espagnon,<sup>37</sup> S. Esumi,<sup>49</sup> D.E. Fields,<sup>34,41</sup> C. Finck,<sup>46</sup> F. Fleuret,<sup>26</sup> S.L. Fokin,<sup>24</sup> B.D. Fox,<sup>41</sup> Z. Fraenkel,<sup>52</sup> J.E. Frantz,<sup>10</sup> A. Franz,<sup>5</sup> A.D. Frawley,<sup>14</sup> Y. Fukao,<sup>25,40,41</sup> S.-Y. Fung,<sup>6</sup> S. Gadrat,<sup>29</sup> M. Germain,<sup>46</sup> A. Glenn,<sup>47</sup> M. Gonin,<sup>26</sup> J. Gosset,<sup>11</sup> Y. Goto,<sup>40,41</sup> R. Granier de Cassagnac,<sup>26</sup> N. Grau,<sup>19</sup> S.V. Greene,<sup>50</sup> M. Grosse Perdekamp,<sup>18,41</sup> H.-Å. Gustafsson,<sup>30</sup> T. Hachiya,<sup>16</sup> J.S. Haggerty,<sup>5</sup> H. Hamagaki,<sup>8</sup> A.G. Hansen,<sup>28</sup> E.P. Hartouni,<sup>27</sup> M. Harvey,<sup>5</sup> K. Hasuko,<sup>40</sup> R. Hayano,<sup>8</sup> X. He,<sup>15</sup> M. Heffner,<sup>27</sup> T.K. Hemmick,<sup>45</sup> J.M. Heuser,<sup>40</sup> P. Hidas,<sup>22</sup> H. Hiejima,<sup>18</sup> J.C. Hill,<sup>19</sup> R. Hobbs,<sup>34</sup> W. Holzmann,<sup>44</sup> K. Homma,<sup>16</sup> B. Hong,<sup>23</sup> A. Hoover,<sup>35</sup> T. Horaguchi,<sup>40,41,48</sup> T. Ichihara,<sup>40,41</sup> V.V. Ikonnikov,<sup>24</sup> K. Imai,<sup>25,40</sup> M. Inaba,<sup>49</sup> M. Inuzuka,<sup>8</sup> D. Isenhower,<sup>1</sup> L. Isenhower,<sup>1</sup> M. Ishihara,<sup>40</sup> M. Issah,<sup>44</sup> A. Isupov,<sup>20</sup> B.V. Jacak,<sup>45</sup> J. Jia,<sup>45</sup> O. Jinnouchi,<sup>40,41</sup> B.M. Johnson,<sup>5</sup> S.C. Johnson,<sup>27</sup> K.S. Joo,<sup>32</sup> D. Jouan,<sup>37</sup> F. Kajihara,<sup>8</sup> S. Kametani,<sup>8,51</sup> N. Kamihara,<sup>40,48</sup> M. Kaneta,<sup>41</sup> J.H. Kang,<sup>53</sup> K. Katou,<sup>51</sup> T. Kawabata,<sup>8</sup> A.V. Kazantsev,<sup>24</sup> S. Kelly,<sup>9,10</sup> B. Khachaturov,<sup>52</sup> A. Khanzadeev,<sup>39</sup> J. Kikuchi,<sup>51</sup> D.J. Kim,<sup>53</sup> E. Kim,<sup>43</sup> G.-B. Kim,<sup>26</sup> H.J. Kim,<sup>53</sup> E. Kinney,<sup>9</sup> A. Kiss,<sup>13</sup> E. Kistenev,<sup>5</sup> A. Kiyomichi,<sup>40</sup> C. Klein-Boesing,<sup>31</sup> H. Kobayashi,<sup>41</sup> L. Kochenda,<sup>39</sup> V. Kochetkov,<sup>17</sup> R. Kohara,<sup>16</sup> B. Komkov,<sup>39</sup> M. Konno,<sup>49</sup> D. Kotchetkov,<sup>6</sup> A. Kozlov,<sup>52</sup> P.J. Kroon,<sup>5</sup> C.H. Kuberg,<sup>1,\*</sup> G.J. Kunde,<sup>28</sup> K. Kurita,<sup>40</sup> M.J. Kweon,<sup>23</sup> Y. Kwon,<sup>53</sup> G.S. Kyle,<sup>35</sup> R. Lacey,<sup>44</sup> J.G. Lajoie,<sup>19</sup> Y. Le Bornec,<sup>37</sup> A. Lebedev,<sup>19,24</sup> S. Leckey,<sup>45</sup> D.M. Lee,<sup>28</sup> M.J. Leitch,<sup>28</sup> M.A.L. Leite,<sup>42</sup> X.H. Li,<sup>6</sup> H. Lim,<sup>43</sup> A. Litvinenko,<sup>20</sup> M.X. Liu,<sup>28</sup> C.F. Maguire,<sup>50</sup> Y.I. Makdisi,<sup>5</sup> A. Malakhov,<sup>20</sup> V.I. Manko,<sup>24</sup> Y. Mao,<sup>38,40</sup> G. Martinez,<sup>46</sup> H. Masui,<sup>49</sup> F. Matathias,<sup>45</sup> T. Matsumoto,<sup>8,51</sup> M.C. McCain,<sup>1</sup> P.L. McGaughey,<sup>28</sup> Y. Miake,<sup>49</sup> T.E. Miller,<sup>50</sup> A. Milov,<sup>45</sup> S. Mioduszewski,<sup>5</sup> G.C. Mishra,<sup>15</sup> J.T. Mitchell,<sup>5</sup> A.K. Mohanty,<sup>4</sup> D.P. Morrison,<sup>5</sup> J.M. Moss,<sup>28</sup> D. Mukhopadhyay,<sup>52</sup> M. Muniruzzaman,<sup>6</sup> S. Nagamiya,<sup>21</sup> J.L. Nagle,<sup>9,10</sup> T. Nakamura,<sup>16</sup> J. Newby,<sup>47</sup> A.S. Nyanin,<sup>24</sup> J. Nystrand,<sup>30</sup> E. O'Brien,<sup>5</sup> C.A. Ogilvie,<sup>19</sup> H. Ohnishi,<sup>40</sup> I.D. Ojha,<sup>3,50</sup> H. Okada,<sup>25,40</sup> K. Okada,<sup>40,41</sup> A. Oskarsson,<sup>30</sup> I. Otterlund,<sup>30</sup> K. Oyama,<sup>8</sup> K. Ozawa,<sup>8</sup> D. Pal,<sup>52</sup> A.P.T. Palounek,<sup>28</sup> V. Pantuev,<sup>45</sup> V. Papavassiliou,<sup>35</sup> J. Park,<sup>43</sup> W.J. Park,<sup>23</sup> S.F. Pate,<sup>35</sup> H. Pei,<sup>19</sup> V. Penev,<sup>20</sup> J.-C. Peng,<sup>18</sup> H. Pereira,<sup>11</sup> V. Peresedov,<sup>20</sup> A. Pierson,<sup>34</sup> C. Pinkenburg,<sup>5</sup> R.P. Pisani,<sup>5</sup> M.L. Purschke,<sup>5</sup> A.K. Purwar,<sup>45</sup> J.M. Qualls,<sup>1</sup> J. Rak,<sup>19</sup> I. Ravinovich,<sup>52</sup> K.F. Read,<sup>36,47</sup> M. Reuter,<sup>45</sup> K. Reygers,<sup>31</sup> V. Riabov,<sup>39</sup> Y. Riabov,<sup>39</sup> G. Roche,<sup>29</sup> A. Romana,<sup>26</sup> M. Rosati,<sup>19</sup> S.S.E. Rosendahl,<sup>30</sup> P. Rosnet,<sup>29</sup> V.L. Rykov,<sup>40</sup> S.S. Ryu,<sup>53</sup> N. Saito,<sup>25,40,41</sup> T. Sakaguchi,<sup>8,51</sup> S. Sakai,<sup>49</sup> V. Samsonov,<sup>39</sup> L. Sanfratello,<sup>34</sup> R. Santo,<sup>31</sup> H.D. Sato,<sup>25,40</sup> S. Sato,<sup>5,49</sup> S. Sawada,<sup>21</sup> Y. Schutz,<sup>46</sup> V. Semenov,<sup>17</sup> R. Seto,<sup>6</sup> T.K. Shea,<sup>5</sup> I. Shein,<sup>17</sup> T.-A. Shibata,<sup>40,48</sup> K. Shigaki,<sup>16</sup> M. Shimomura,<sup>49</sup> A. Sickles,<sup>45</sup> C.L. Silva,<sup>42</sup> D. Silvermyr,<sup>28</sup> K.S. Sim,<sup>23</sup> A. Soldatov,<sup>17</sup> R.A. Soltz,<sup>27</sup> W.E. Sondheim,<sup>28</sup> S.P. Sorensen,<sup>47</sup> I.V. Sourikova,<sup>5</sup> F. Staley,<sup>11</sup> P.W. Stankus,<sup>36</sup> E. Stenlund,<sup>30</sup> M. Stepanov,<sup>35</sup> A. Ster,<sup>22</sup> S.P. Stoll,<sup>5</sup> T. Sugitate,<sup>16</sup> J.P. Sullivan,<sup>28</sup> S. Takagi,<sup>49</sup> E.M. Takagui,<sup>42</sup> A. Taketani,<sup>40,41</sup> K.H. Tanaka,<sup>21</sup> Y. Tanaka,<sup>33</sup> K. Tanida,<sup>40</sup> M.J. Tannenbaum,<sup>5</sup> A. Taranenko,<sup>44</sup> P. Tarján,<sup>12</sup> T.L. Thomas,<sup>34</sup> M. Togawa,<sup>25,40</sup> J. Tojo,<sup>40</sup> H. Torii,<sup>25,41</sup> R.S. Towell,<sup>1</sup> V.-N. Tram,<sup>26</sup> I. Tserruya,<sup>52</sup> Y. Tsuchimoto,<sup>16</sup> H. Tydesjö,<sup>30</sup> N. Tyurin,<sup>17</sup> T.J. Uam,<sup>32</sup> H.W. van Hecke,<sup>28</sup> J. Velkovska,<sup>5</sup> M. Velkovsky,<sup>45</sup> V. Veszprémi,<sup>12</sup> A.A. Vinogradov,<sup>24</sup> M.A. Volkov,<sup>24</sup> E. Vznuzdaev,<sup>39</sup> X.R. Wang,<sup>15</sup> Y. Watanabe,<sup>40,41</sup> S.N. White,<sup>5</sup> N. Willis,<sup>37</sup> F.K. Wohn,<sup>19</sup> C.L. Woody,<sup>5</sup> W. Xie,<sup>6</sup> A. Yanovich,<sup>17</sup> S. Yokkaichi,<sup>40,41</sup> G.R. Young,<sup>36</sup> I.E. Yushmanov,<sup>24</sup> W.A. Zajc,<sup>10,†</sup> C. Zhang,<sup>10</sup> S. Zhou,<sup>7</sup> J. Zimányi,<sup>22</sup> L. Zolin,<sup>20</sup> and X. Zong<sup>19</sup>

(PHENIX Collaboration)

<sup>1</sup>Abilene Christian University, Abilene, TX 79699, U.S.

<sup>2</sup>Institute of Physics, Academia Sinica, Taipei 11529, Taiwan

<sup>3</sup>Department of Physics, Banaras Hindu University, Varanasi 221005, India

<sup>4</sup>Bhabha Atomic Research Centre, Bombay 400 085, India

<sup>5</sup>Brookhaven National Laboratory, Upton, NY 11973-5000, U.S.

<sup>6</sup>University of California - Riverside, Riverside, CA 92521, U.S.

- <sup>7</sup>China Institute of Atomic Energy (CIAE), Beijing, People's Republic of China
- <sup>8</sup>Center for Nuclear Study, Graduate School of Science, University of Tokyo, 7-3-1 Hongo, Bunkyo, Tokyo 113-0033, Japan
- <sup>9</sup>University of Colorado, Boulder, CO 80309, U.S.
- <sup>10</sup>Columbia University, New York, NY 10027 and Nevis Laboratories, Irvington, NY 10533, U.S.
- <sup>11</sup>Dapnia, CEA Saclay, F-91191, Gif-sur-Yvette, France
- <sup>12</sup>Debrecen University, H-4010 Debrecen, Egyetem tér 1, Hungary
- <sup>13</sup>ELTE, Eötvös Loránd University, H - 1117 Budapest, Pázmány P. s. 1/A, Hungary
- <sup>14</sup>Florida State University, Tallahassee, FL 32306, U.S.
- <sup>15</sup>Georgia State University, Atlanta, GA 30303, U.S.
- <sup>16</sup>Hiroshima University, Kagamiyama, Higashi-Hiroshima 739-8526, Japan
- <sup>17</sup>IHEP Protvino, State Research Center of Russian Federation, Institute for High Energy Physics, Protvino, 142281, Russia
- <sup>18</sup>University of Illinois at Urbana-Champaign, Urbana, IL 61801, U.S.
- <sup>19</sup>Iowa State University, Ames, IA 50011, U.S.
- <sup>20</sup>Joint Institute for Nuclear Research, 141980 Dubna, Moscow Region, Russia
- <sup>21</sup>KEK, High Energy Accelerator Research Organization, Tsukuba, Ibaraki 305-0801, Japan
- <sup>22</sup>KFKI Research Institute for Particle and Nuclear Physics of the Hungarian Academy of Sciences (MTA KFKI RMKI), H-1525 Budapest 114, POBox 49, Budapest, Hungary
- <sup>23</sup>Korea University, Seoul, 136-701, Korea
- <sup>24</sup>Russian Research Center "Kurchatov Institute", Moscow, Russia
- <sup>25</sup>Kyoto University, Kyoto 606-8502, Japan
- <sup>26</sup>Laboratoire Leprince-Ringuet, Ecole Polytechnique, CNRS-IN2P3, Route de Saclay, F-91128, Palaiseau, France
- <sup>27</sup>Lawrence Livermore National Laboratory, Livermore, CA 94550, U.S.
- <sup>28</sup>Los Alamos National Laboratory, Los Alamos, NM 87545, U.S.
- <sup>29</sup>LPC, Université Blaise Pascal, CNRS-IN2P3, Clermont-Fd, 63177 Aubiere Cedex, France
- <sup>30</sup>Department of Physics, Lund University, Box 118, SE-221 00 Lund, Sweden
- <sup>31</sup>Institut für Kernphysik, University of Muenster, D-48149 Muenster, Germany
- <sup>32</sup>Myongji University, Yongin, Kyonggido 449-728, Korea
- <sup>33</sup>Nagasaki Institute of Applied Science, Nagasaki-shi, Nagasaki 851-0193, Japan
- <sup>34</sup>University of New Mexico, Albuquerque, NM 87131, U.S.
- <sup>35</sup>New Mexico State University, Las Cruces, NM 88003, U.S.
- <sup>36</sup>Oak Ridge National Laboratory, Oak Ridge, TN 37831, U.S.
- <sup>37</sup>IPN-Orsay, Université Paris Sud, CNRS-IN2P3, BP1, F-91406, Orsay, France
- <sup>38</sup>Peking University, Beijing, People's Republic of China
- <sup>39</sup>PNPI, Petersburg Nuclear Physics Institute, Gatchina, Leningrad region, 188300, Russia
- <sup>40</sup>RIKEN (The Institute of Physical and Chemical Research), Wako, Saitama 351-0198, JAPAN
- <sup>41</sup>RIKEN BNL Research Center, Brookhaven National Laboratory, Upton, NY 11973-5000, U.S.
- <sup>42</sup>Universidade de São Paulo, Instituto de Física, Caixa Postal 66318, São Paulo CEP05315-970, Brazil
- <sup>43</sup>System Electronics Laboratory, Seoul National University, Seoul, South Korea
- <sup>44</sup>Chemistry Department, Stony Brook University, SUNY, Stony Brook, NY 11794-3400, U.S.
- <sup>45</sup>Department of Physics and Astronomy, Stony Brook University, SUNY, Stony Brook, NY 11794, U.S.
- <sup>46</sup>SUBATECH (Ecole des Mines de Nantes, CNRS-IN2P3, Université de Nantes) BP 20722 - 44307, Nantes, France
- <sup>47</sup>University of Tennessee, Knoxville, TN 37996, U.S.
- <sup>48</sup>Department of Physics, Tokyo Institute of Technology, Oh-okayama, Meguro, Tokyo 152-8551, Japan
- <sup>49</sup>Institute of Physics, University of Tsukuba, Tsukuba, Ibaraki 305, Japan
- <sup>50</sup>Vanderbilt University, Nashville, TN 37235, U.S.
- <sup>51</sup>Waseda University, Advanced Research Institute for Science and Engineering, 17 Kikui-cho, Shinjuku-ku, Tokyo 162-0044, Japan
- <sup>52</sup>Weizmann Institute, Rehovot 76100, Israel
- <sup>53</sup>Yonsei University, IPAP, Seoul 120-749, Korea
- (Dated: October 8, 2018)

PHENIX has measured the centrality dependence of mid-rapidity pion, kaon and proton transverse momentum distributions in d+Au and p+p collisions at  $\sqrt{s_{NN}} = 200$  GeV. The p+p data provide a reference for nuclear effects in d+Au and previously measured Au+Au collisions. Hadron production is enhanced in d+Au, relative to independent nucleon-nucleon scattering, as was observed in lower energy collisions. The nuclear modification factor for (anti) protons is larger than that for pions. The difference increases with centrality, but is not sufficient to account for the abundance of baryon production observed in central Au+Au collisions at RHIC. The centrality dependence in d+Au shows that the nuclear modification factor increases gradually with the number of collisions suffered by each participant nucleon. We also present comparisons with lower energy data as well as with parton recombination and other theoretical models of nuclear effects on particle production.

## I. INTRODUCTION

Since the early 1970's, it is well established [1, 2, 3], that energetic particle production in proton-nucleus (p+A) collisions increases faster than the number of binary nucleon-nucleon collisions. This effect, called the ‘‘Cronin effect’’, is a manifestation of the fact that particle production and propagation is influenced by the nucleus. If the A-dependence of the invariant cross section,  $I$ , of particle  $i$  in p+A collisions is parameterized as

$$I_i(p_T, A) = I_i(p_T, 1) \cdot A^{\alpha_i(p_T)} \quad (1)$$

then it has been observed that  $\alpha_i$  is greater than unity above some transverse momentum value, typically 1-1.5 GeV/c, denoting significant enhancement of particle production in p+A collisions. The enhancement depends on the momentum and the type of particle produced, with protons and antiprotons exhibiting a much larger enhancement than pions and kaons at  $p_T > 2 - 3$  GeV/c. At  $\sqrt{s_{NN}} = 27.4$  GeV, the enhancement peaks at around  $p_T=4.5$  GeV/c, with  $\alpha_{K^+} \simeq \alpha_{\pi^+} = 1.109 \pm 0.007$ , while, at the same momentum, the protons can be described by an  $\alpha$ -factor of  $\alpha_p - \alpha_{\pi^+} = 0.231 \pm 0.013$  [2].

Although the observables in Eq. 1 have been clearly related to the nuclear medium, the cause of the Cronin enhancement and its species dependence are not yet completely understood and further experimental study is warranted in its own right. Furthermore, in the search for the Quark Gluon Plasma at the Relativistic Heavy Ion Collider (RHIC), the Cronin effect is extremely important, as novel effects observed in central Au+Au collisions require good control of the initial state conditions. At RHIC energies, it was discovered that hadron production at high transverse momentum ( $p_T \geq 2$  GeV/c) is suppressed in central Au+Au collisions [4] compared to nucleon-nucleon collisions. Such suppression may be interpreted as a consequence of the energy loss suffered by the hard-scattered partons as they propagate through the hot and dense medium. However, since the Cronin effect acts in the opposite direction enhancing the hadron yields, it has to be taken into account when the parton energy loss is determined from the data.

Another discovery at RHIC, originally unexpected, is that the yields of  $p$  and  $\bar{p}$  at intermediate  $p_T$  ( $1.5 < p_T < 5$  GeV/c) in central Au+Au collisions [5, 6, 7] are comparable to the yield of pions, in striking contrast to the proton to pion ( $p/\pi$ ) ratios of  $\sim 0.1 - 0.3$  measured in p+p collisions [8]. Novel mechanisms of particle production in the environment of dense matter, such as recombination of boosted quarks [9] or contributions from baryon junctions [10], which can become dominant in the presence of pion suppression were proposed to explain the

data. Since it has been observed that at lower energies Cronin enhancement is stronger for protons than for pions [2], this effect has to be considered at RHIC before new physics is invoked.

The effects from the initial state are best studied by performing a control experiment in which no hot and dense matter is produced. Deuteron + gold collisions at  $\sqrt{s_{NN}}= 200$  GeV serve this purpose. Since there is no hot and dense final state medium, the initial state conditions become accessible to the experiment. In addition to Cronin enhancement, known initial state effects also include nuclear shadowing and gluon saturation [11]. The Cronin enhancement is usually attributed to momentum broadening due to multiple initial state soft [12] or semi-hard [13, 14, 15, 16] scattering. Such models typically do not predict the particle species dependence observed in the data. Recently, Hwa and collaborators provided an alternative explanation due to final state interactions. The particle species dependent enhancement is attributed to recombination of shower quarks with those from the medium, where no distinction is made if hot or cold nuclear matter is produced [17]. Identified hadron production measured as a function of centrality brings important experimental data relevant to the long outstanding problem of the baryon Cronin effect. The dependence of the enhancement upon the thickness of the medium, or the number of collisions suffered by each participating nucleon, can help differentiate among the different scattering models, and the species dependence helps to separate initial from final state effects in d+Au.

The paper is arranged as follows. Section II describes the experiment, data analysis, and systematic uncertainties. Section III presents hadron spectra, yields and the resulting nuclear modification factors. Discussion of the centrality, energy and species dependence of the nuclear modification factors and implications for understanding of the Cronin effect are in section IV. Section V presents conclusions.

## II. EXPERIMENT AND DATA ANALYSIS

### A. Data Sets and Trigger

Data presented here include collisions at  $\sqrt{s_{NN}} = 200$  GeV of Au+Au taken in the 2002 run of RHIC and d+Au and p+p collected in 2003. In the following we discuss analysis of the p+p and d+Au data; details of the Au+Au analysis, and the Au+Au results, are found in [7]. Events with vertex position along the beam axis within  $|z| < 30$  cm were triggered by the Beam-Beam Counters (BBC) located at  $|\eta| = 3.0-3.9$  [18]. The minimum bias trigger accepts  $88.5 \pm 4\%$  of all d+Au collisions that satisfy the vertex condition, and  $51.6 \pm 9.8\%$  of p+p collisions. A total of  $42 \times 10^6$  minimum bias d+Au events and  $25 \times 10^6$  minimum bias p+p events were analyzed.

In p+p collisions, PHENIX determines the differential

\*Deceased

†PHENIX Spokesperson:zajc@nevis.columbia.edu

TABLE I: Mean number of binary collisions, participating nucleons from the Au nucleus, number of collisions per participating deuteron nucleon, and trigger bias corrections for the d+Au centrality bins.

	00-20%	20-40%	40-60%	60-88%
$\langle N_{coll} \rangle$	15.4±1.0	10.6±0.7	7.0±0.6	3.1±0.3
$\langle N_{part} \rangle$	15.6±0.9	11.1±0.6	7.7±0.4	4.2±0.3
$\langle \nu = N_{coll}/N_{part}^d \rangle$	7.5±0.5	5.6±0.4	4.0±0.3	2.2±0.2
Trigger bias correction	0.95±0.3	0.99±0.007	1.03±0.009	1.04±0.027

invariant cross section via

$$E \frac{d^3\sigma}{dp^3} = \frac{\sigma_{BBC}}{N_{BBC}^{Total}} \cdot \frac{1}{2\pi} \cdot \frac{1}{p_T} \cdot C_{eff}^{geo}(p_T) \cdot C_{bias}^{BBC} \cdot \frac{d^2N}{dp_T dy} \quad (2)$$

The BBC cross section  $\sigma_{BBC}$  was determined via the van der Meer scan technique [19]. In this p+p data set,  $\sigma_{BBC} = 23.0 \pm 2.2$  (9.6%) mb.  $N_{BBC}^{Total}$  is the total number of BBC triggers analyzed. The factor  $C_{eff}^{geo}(p_T)$  denotes the efficiency and geometrical acceptance correction, calculated with a detailed GEANT Monte Carlo simulation [20] of the PHENIX detector.  $C_{eff}^{geo}(p_T)$  normalizes the cross section in one unit of rapidity and full azimuthal coverage. The  $C_{bias}^{BBC}$  factor corrects for the fact that the forward BBC trigger counters measure only a fraction of the inelastic p+p cross section. This subset of events on which the BBC triggers contains only a fraction of the inclusive particle yield at mid-rapidity. For charged hadrons this fraction was determined using triggers on the beam crossing clock; the fraction was found to be  $0.80 \pm 0.02$ , independent of  $p_T$ . The  $C_{bias}^{BBC}$  term is, in our nomenclature, the inverse of this fraction.

In d+Au collisions PHENIX measures the inelastic yield per BBC triggered event.<sup>1</sup> The collision centrality is selected in d+Au using the south (Au-going side) BBC (BBCS). We assume that the BBCS signal is proportional to the number of participating nucleons ( $N_{part}^{Au}$ ) in the Au nucleus, and that the hits in the BBCS are uncorrelated to each other. We use a Glauber model [22] and simulation of the BBC to define 4 centrality classes in d+Au collisions, as discussed in detail in [23]. The deuteron nucleus is modeled after a wave function due to Hulthén [24]

$$\phi_d(\mathbf{r}_{pn}) = \left( \frac{\alpha\beta(\alpha + \beta)}{2\pi(\alpha - \beta)^2} \right)^{\frac{1}{2}} (e^{-\alpha r_{pn}} - e^{-\beta r_{pn}})/r_{pn} \quad (3)$$

where  $\alpha = 0.228 \text{ fm}^{-1}$  and  $\beta = 1.18 \text{ fm}^{-1}$  and  $\mathbf{r}_{np}$  refers to the separation between the proton and the neutron. The Au nucleus is modeled using a Woods-Saxon density

distribution

$$\rho(r) = \frac{\rho_0}{1 + \exp\left(\frac{r-c}{a}\right)} \quad (4)$$

where  $a = 0.54 \text{ fm}$  and  $c = 1.12 \times A^{1/3} - 0.86 \times A^{-1/3} = 6.40 \text{ fm}$ , a value which agrees well with the measured charge radius of  $R = 6.38 \text{ fm}$  for gold.

Using the above parameters and taking into account the BBC efficiency the mean number of binary collisions along with the mean number of participating nucleons from the Au nucleus that correspond to each centrality bin are shown in Table I. For the minimum bias d+Au collisions,  $\langle N_{coll} \rangle = 8.5 \pm 0.4$  and  $\langle N_{part} \rangle = 9.1 \pm 0.4$ .

As for p+p collisions, there is a BBC trigger bias, but it is much smaller in d+Au. In addition, a second bias occurs in d+Au centrality selected collisions. This second bias arises from the fact that events containing high  $p_T$  hadrons from hard scatterings may have larger multiplicity, and consequently produce a larger signal in the BBCS. Such events would be considered more central than events without a hard scattering. This effect gives an opposite bias from the first trigger bias effect in the most peripheral bin as events can be shifted out of this bin but not into it. We correct for both biases in d+Au collisions using simulations and a Glauber model. The combined corrections for these effects range from 0-5%, depending on the centrality category, and are shown in Table I. Systematic uncertainties on these corrections are less than 4%.

## B. Tracking and Particle Identification

Charged particles are reconstructed using a drift chamber (DC) and two layers of multi-wire proportional chambers with pad readout (PC1, PC3) [18]. Pattern recognition is based on a combinatorial Hough transform in the track bend plane, while the polar angle is determined by PC1 and the location of the collision vertex along the beam direction [25]. The track reconstruction efficiency is approximately 98%.

Particle momenta are measured with a resolution  $\delta p/p = 0.7\% \oplus 1.1\% p \text{ (GeV}/c)$ . The momentum scale is known to 0.7%. Particle identification is based on particle mass calculated from the measured momentum and the velocity obtained from the time-of-flight and path length along the trajectory. The measurement uses the

<sup>1</sup> To convert the reported inelastic yield to differential cross section, one must multiply by the beam-beam trigger cross section of  $\sigma_{MB}^{tot}(dAu)\epsilon_{MB}^{BBC}(dAu) = 1.99 \pm 0.10\text{b}$  [21].

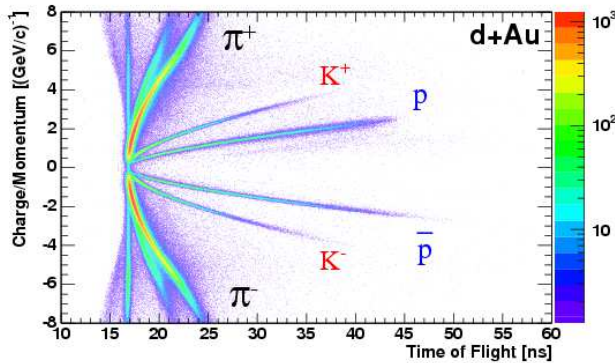


FIG. 1: (color online) Time of flight vs. charge/momentum for particles in minimum bias d+Au collisions. Bands corresponding to the different hadrons are labeled. Electron and muon bands are also visible, though not labeled.

portion of the spectrometer containing the high resolution time-of-flight (TOF) detector, which covers pseudorapidity  $-0.35 \leq \eta \leq 0.35$  and  $\Delta\phi = \pi/8$  in azimuthal angle. The timing uses the BBC for the global start, and stop signals from the TOF scintillators located at a radial distance of 5.06 m. Tracks are required to match a hit on the TOF within  $\pm 3$  standard deviations ( $\sigma$ ) of the track projection to the TOF radial location. The particle yields are corrected for losses due to this matching cut.

Figure 1 illustrates the performance of the hadron identification system. The system resolution is  $\sigma \approx 130$  ps for both d+Au and p+p; the start time resolution is limited by the low hit multiplicity in the BBC. The TOF resolution achieved allows for a clear separation of  $\pi/K$  and  $K/p$  up to  $p_T = 2$  GeV/c and  $p_T = 3.6$  GeV/c, respectively. A  $2\sigma$  cut in mass squared is used to separate the different hadron species, as shown in Fig. 2 for hadrons in the  $p_T$  range from 1.2 - 1.6 GeV/c. A clear separation between pions and kaons is seen. The particle yields are corrected for losses due to the  $2\sigma$  cut.

Corrections to the charged particle spectrum for geometrical acceptance, decays in flight, reconstruction efficiency, energy loss in detector material, and momentum resolution are determined using a single-particle GEANT Monte Carlo simulation.

The proton and antiproton spectra are corrected for feed-down from weak decays via a Monte Carlo simulation using as input experimental data on  $\Lambda$  production. The total number of protons produced in the collisions can be written as:  $p + 0.64(\Lambda + \Sigma^0 + \Xi^0 + \Xi^- + \Omega^-) + 0.52\Sigma^+$  where  $p$  denotes the primordial number of protons produced, and the other symbols denote the primordial number of those particles produced in the collision. 0.64 and 0.52 are the branching ratios for  $\Lambda \rightarrow p\pi^-$  and  $\Sigma^+ \rightarrow p\pi^0$ , respectively. The hyperons listed together with  $\Lambda$  decay to  $\Lambda$  with approximately 100% branching

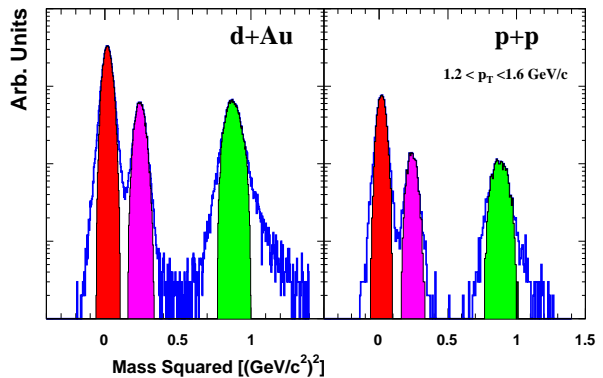


FIG. 2: (color online) Mass squared distribution for positively charged tracks with  $1.2 \leq p_T \leq 1.6$  GeV/c, using the high resolution time-of-flight measurement. The solid regions indicate the mass squared ranges for accepted pions, kaons and protons, respectively, from left to right.

ratio, and so yield protons with the  $\Lambda \rightarrow p\pi$  branching ratio. We estimate the proton and antiproton spectra from weak decays and subtract them from the measured yields, using experimental data from UA5 [26] from non-single diffractive  $\sqrt{s} = 200$  GeV  $p+\bar{p}$  collisions, and preliminary  $\Lambda$  and  $\bar{\Lambda}$  spectra from STAR in p+p and d+Au collisions at the same energy [27, 28, 29, 30]. The shape of the  $\Sigma^0$ ,  $\Xi^0$ , and  $\Xi^-$  spectra are constructed from the  $\Lambda$  spectrum by  $m_T$  scaling (i.e. under the assumption that these hadrons are all produced with roughly the same spectrum in transverse mass [30]). The relative normalization of  $\Lambda$ ,  $\Sigma^0$ ,  $\Xi^0$ , and  $\Xi^-$  from UA5 [26] is used for both p+p and d+Au collisions. This is justified by the similarity of the Cronin effect for different baryons. The contribution of  $\Omega^-$  is negligible, and is not included in the correction. The Monte Carlo simulation decays these baryons and propagates the products through the PHENIX magnetic field and central arm detectors, accounting also for the change of momentum distributions between parent and daughter particles due to decay kinematics. The resulting proton and antiproton spectra are then subtracted from the measured inclusive spectra. The fractional contribution from feed-down protons from weak decays to the total measured proton spectrum,  $f$ , is approximately 30% at moderate and high  $p_T$  growing slowly for lower  $p_T$  and reaching 40% at  $p_T = 0.6$  GeV/c.  $f$  is shown as a function of  $p_T$  in Fig. 3, along with the corresponding fractional contribution for the antiprotons.

### C. Systematic Uncertainties

Systematic uncertainties on the hadron spectra are estimated as in reference [7]. Various sets of  $p_T$  spectra and ratios of different particle types were made by vary-

TABLE II: Systematic errors in percent on particle yields in d+Au and p+p collisions. These values are independent of  $p_T$ .

	d+Au	p+p
geometric acceptance correction	4	4
track matching	9	8
timing variations	5	5
reconstruction efficiency correction	3	4
energy loss correction	1	2
trigger bias	-	4

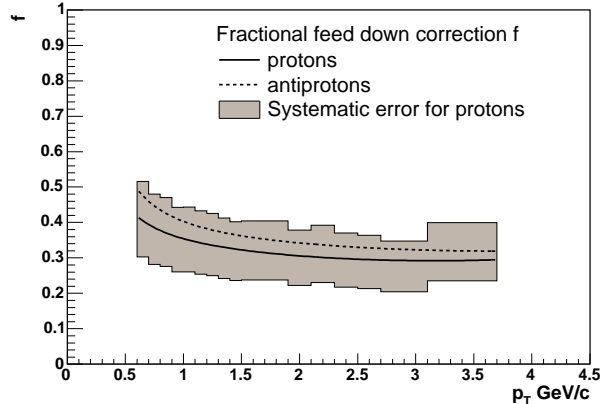


FIG. 3: Fractional contributions of protons,  $f$ , (solid line) and antiprotons (dashed line), as a function of  $p_T$ , from weak decays in all measured protons and antiprotons. Systematic error band (26%) for the protons is shown and discussed in the text. The same systematic error applies for the antiprotons.

ing the cut parameters such as fiducial cut to check acceptance corrections, track association (i.e. matching) windows, and PID cuts, from those used in the analysis. For each of these spectra and ratios the same changes in cuts were made in the Monte Carlo analysis. The uncertainties were evaluated by comparing fully corrected spectra and ratios from different cuts. The resulting uncertainties from each cut are given in Table II and added in quadrature to yield overall systematic uncertainties.

Additional systematic uncertainties on the hadron spectra arise from time variations in the TOF timing (slat-by-slat and run-by-run variations), the small remaining contamination by other species after matching and PID cuts, uncertainty in the corrections for track reconstruction efficiency, and uncertainty on particle energy loss in the detector material. These uncertainties, which do not depend measurably on the hadron momentum, are listed in Table II. The sizable uncertainty in the matching cut is due to the non-Gaussian tails on the  $z$ -coordinate matching distributions. The track matching in this direction is limited by a relatively poor vertex resolution determined by the BBC in p+p and d+Au collisions due to the small multiplicities. The quoted 3%

4% uncertainty in the reconstruction efficiency correction represents the maximum local discrepancy between efficiencies measured with strict and loose track quality cuts.

Uncertainties due to particle identification cuts are momentum dependent. For protons and antiprotons, the identification uncertainty is 8% at low  $p_T$  and decreases to 3% at high  $p_T$ . Kaons at low momentum have 10% PID uncertainty, decreasing to 3% at high  $p_T$ . For pions the uncertainty increases from 4% to 10% with increasing  $p_T$ . Kaon and proton uncertainties decrease with increasing  $p_T$  because energy loss and decay corrections become smaller. The pion uncertainties are dominated by the particle identification performance, which worsens with increasing  $p_T$ .

The systematic error on the feed-down proton spectrum is 26%, primarily due to uncertainty in the measured  $\Lambda$  spectra and particle composition. The resulting systematic error on the final prompt proton and antiproton spectra is of the order of 10% in both p+p and d+Au. The systematic error on the proton to pion ratio is 12%, including the uncertainty on  $\bar{\Lambda}/\Lambda$ .

Systematic uncertainties on the d+Au nuclear modification factors mostly cancel as the p+p and d+Au data were collected immediately following one another, and detector performance was very similar. The overall systematic error in the nuclear modification factor is due to uncertainties in the reconstruction efficiencies, fiducial volumes, and small run-by-run variations. It is approximately 10%, independent of particle species and  $p_T$ . An additional d+Au scale uncertainty is shown as boxes around 1.0 in the figures; this is the quadrature sum of uncertainties on the p+p cross section of 9.6%, and the number of binary collisions in the each centrality bin (presented in Table I).

The systematic error on the Au+Au nuclear modification factors is derived by propagating the systematic errors on p+p and Au+Au data [7] to the final ratio. The average systematic error for pions is approximately 15%, while for protons and antiprotons it is on the order of 19%. The normalization uncertainty, as in d+Au, is the quadrature sum of uncertainties on the p+p cross section and the error on the number of binary collisions in the corresponding Au+Au centrality bin from reference [7]. We note that for the most central Au+Au bin (0-5%),  $N_{coll}=1065.4$  and the uncertainty is  $\pm 105.3$ ; in the most peripheral bin (60-92%),  $N_{coll}=14.5 \pm 4.0$ .

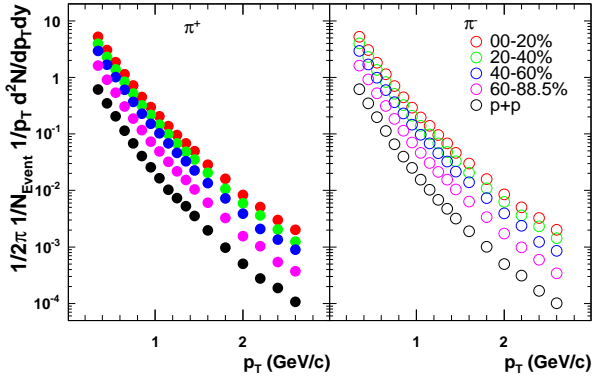


FIG. 4: (color online) Invariant yields at mid-rapidity for positive and negative pions as a function of  $p_T$  for various centrality classes in d+Au and p+p collisions. The error bars show statistical uncertainties only and are typically smaller than the data points.

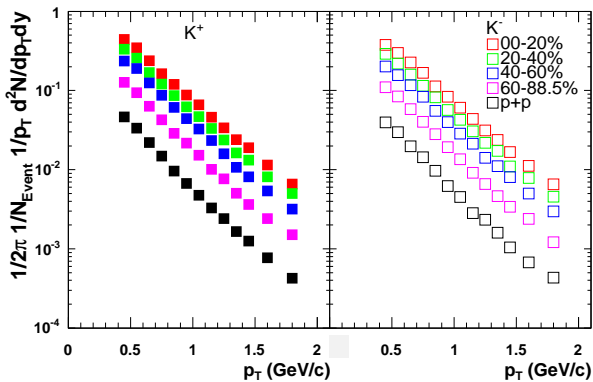


FIG. 5: (color online) Invariant yields at mid-rapidity for positive and negative kaons as a function of  $p_T$  for various centrality classes in d+Au and p+p collisions. The error bars show statistical uncertainties only and are typically smaller than the data points.

### III. RESULTS

#### A. Hadron spectra

The fully corrected  $p_T$  distributions of  $\pi$ ,  $K$ ,  $p$ , and  $\bar{p}$  for the four d+Au centrality bins and for p+p collisions are shown in Figures 4, 5, and 6, respectively. Pions show a power law spectral shape, while kaons and protons are exponential.

In order to probe the hadron production mechanism, it is instructive to compare particle and anti-particle spectra. Figures 7, 8, and 9 show the ratios of antiparticle

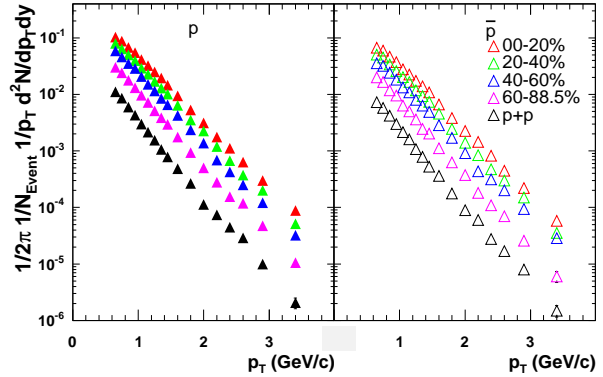


FIG. 6: (color online) Invariant yields at mid-rapidity for protons and antiprotons as a function of  $p_T$  for various centrality classes in d+Au and p+p collisions. The error bars show statistical uncertainties only and are typically smaller than the data points.

to particle production as a function of  $p_T$  in p+p, d+Au and, for comparison, central Au+Au collisions from reference [7] for  $\pi$ ,  $K$  and  $p$ , respectively. For all three hadron species the ratios are flat with  $p_T$ . d+Au yield ratios are in good agreement with p+p collisions, and the ratios remain the same even in central Au+Au collisions. The production ratio of antiparticle to particle is  $0.99 \pm 0.01(\text{stat}) \pm 0.06(\text{syst})$  for pions and  $0.92 \pm 0.01(\text{stat}) \pm 0.07(\text{syst})$  for kaons in both minimum bias d+Au and p+p collisions. The antiproton to proton ratio is measured to be  $0.70 \pm 0.01(\text{stat}) \pm 0.08(\text{syst})$  in minimum bias d+Au collisions and  $0.71 \pm 0.01(\text{stat}) \pm 0.08(\text{syst})$  in p+p collisions. All ratios are consistent within errors with values reported by PHOBOS [31] and BRAHMS [32].

#### B. Nuclear Modification Factors

The measurement of identified hadrons in both d+Au and p+p collisions allows study of the centrality dependence of the nuclear modification factor in d+Au. A standard way to quantify nuclear medium effects on high  $p_T$  particle production in nucleus-nucleus collisions is provided by the *nuclear modification factor*. This is the ratio of the d+A invariant yields to the binary collision scaled p+p invariant yields:

$$R_{dA}(p_T) = \frac{(1/N_{dA}^{evt}) d^2 N_{dA}/dy dp_T}{T_{dAu} d^2 \sigma_{inel}^{pp}/dy dp_T}, \quad (5)$$

where  $T_{dAu} = \langle N_{coll} \rangle / \sigma_{inel}^{pp}$  describes the nuclear geometry, and  $d^2 \sigma_{inel}^{pp}/dy dp_T$  for p+p collisions is derived from the measured p+p cross section.  $\langle N_{coll} \rangle$  is the average number of inelastic nucleon-nucleon collisions determined



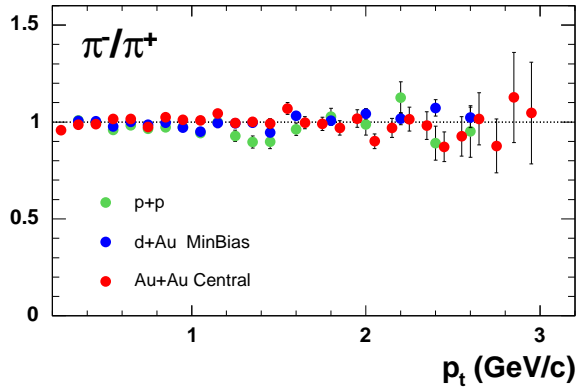


FIG. 7: (color online) Ratio of mid-rapidity spectra for  $\pi^-$  to  $\pi^+$  in d+Au, p+p and central Au+Au collisions. The error bars show statistical uncertainties only.

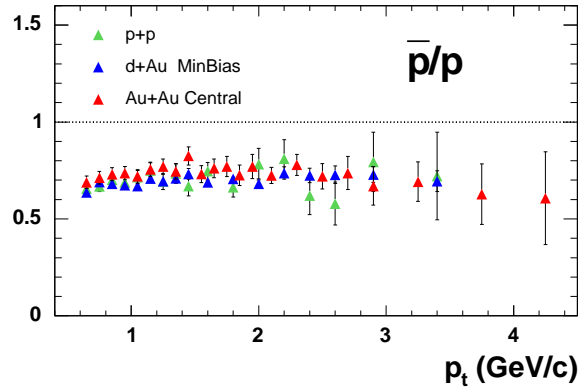


FIG. 9: (color online) Ratio of mid-rapidity spectra for antiprotons to protons in d+Au, p+p and central Au+Au collisions [7]. The error bars show statistical uncertainties only.

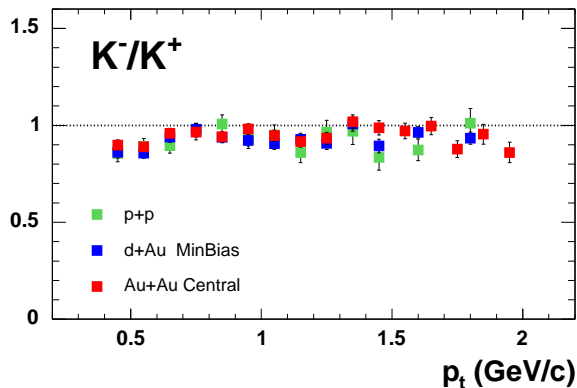


FIG. 8: (color online) Ratio of mid-rapidity spectra for  $K^-$  to  $K^+$  in d+Au, p+p and central Au+Au collisions. The error bars show statistical uncertainties only.

from simulation using the Glauber model as input, as described in section II A.  $N_{dA}^{evt}$  is the number of d+Au events in the relevant centrality class.

Figure 10 shows  $R_{dA}$  for pions, kaons and protons for minimum bias d+Au collisions. We observe a nuclear enhancement in the production of hadrons with  $p_T \geq 1.5 - 2$  GeV/c in d+Au collisions, compared to that in p+p. As was already suggested when comparing the enhancement for inclusive charged hadrons with that of neutral pions [33], there is a species dependence in the Cronin effect. The Cronin effect for charged pions is small, as was observed for neutral pions. The nuclear enhancement for protons and antiprotons is considerably larger. The kaon measurement has a more limited kinematic range, but the  $R_{dA}$  is in agreement with that of the pions at comparable  $p_T$ .

Figure 11 shows  $R_{dA}$  for pions, kaons and protons in

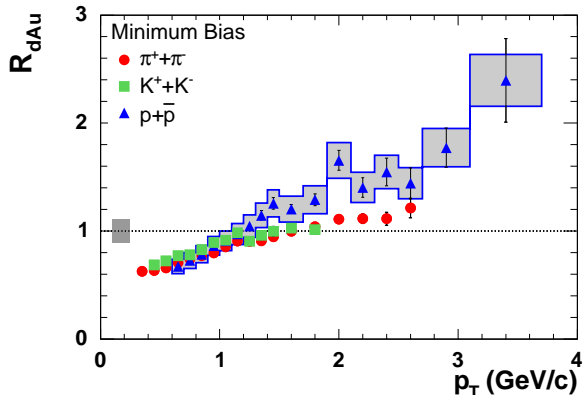


FIG. 10: (color online) Nuclear modification factor  $R_{dA}$  for pions, kaons and protons in d+Au collisions for minimum bias events. The error bars represent the statistical errors. The box around 1.0 shows uncertainties in the p+p absolute cross section and in the calculation of  $N_{coll}$ . For the proton and antiproton  $R_{dA}$ , the  $\sim 10\%$  systematic uncertainty is also presented as boxes around the points. The systematic uncertainty on the pion and kaon  $R_{dA}$  is similar but not shown in the picture for clarity.

the four d+Au centrality bins. Peripheral d+Au collisions ( $\langle N_{coll} \rangle = 3.1 \pm 0.3$ ) do not show any modification of high momentum hadron production, compared to that in p+p collisions. At  $p_T \leq 1$  GeV/c, the nuclear modification factor falls below 1.0. This is to be expected as soft particle production scales with the number of participating nucleons, not with the number of binary nucleon-nucleon collisions. More central collisions show increasing nuclear enhancement in both high  $p_T$  pion and proton production.

The bands in Fig. 11 show a calculation of the Cronin



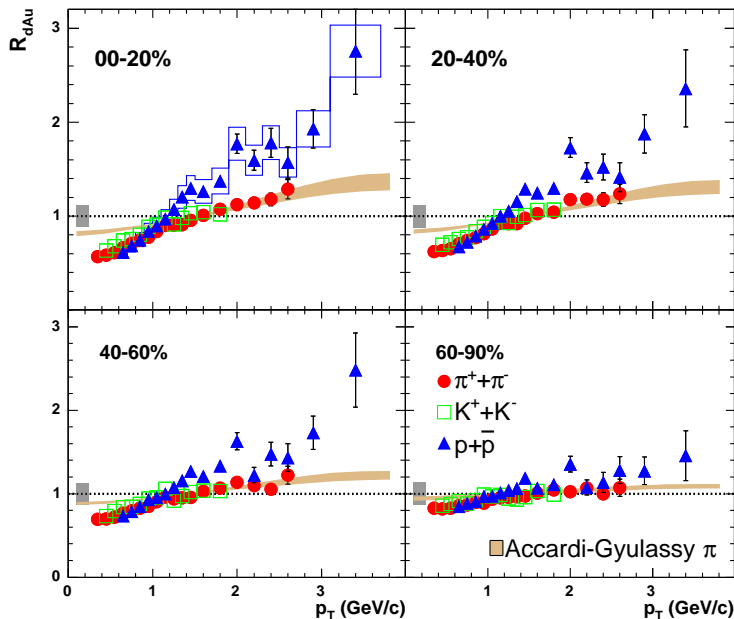


FIG. 11: (color online) Nuclear modification factor  $R_{dAu}$  for pions, kaons and protons in d+Au collisions in four centrality bins. The error bars represent the statistical errors. Boxes around 1.0 show uncertainties in the p+p absolute cross section and in the calculation of  $N_{coll}$ . For the proton and antiproton  $R_{dA}$ , the  $\sim 10\%$  systematic uncertainty is also presented as boxes around the points. The systematic uncertainty on the pion and kaon  $R_{dA}$  is similar but not shown in the picture for clarity. Solid bands show the calculation of the nuclear modification factors for pions by Accardi and Gyulassy [13].

effect for pions by Accardi and Gyulassy, using a pQCD model of multiple semi-hard collisions and taking geometrical shadowing into account [13]. The agreement above 1 GeV/c, where the calculation should be reliable, is very good for all four centrality bins. This agreement illustrates that the multiple partonic scattering and nuclear shadowing alone can explain the observed Cronin effect and leaves very little room for gluon saturation effects in the nuclear initial state at mid-rapidity at RHIC [13].

### C. Centrality Dependence

We further probe the effect of cold nuclear matter upon the hadron production using the number of collisions suffered by each projectile nucleon for the four centrality bins. Figure 12 compares the centrality dependence of  $R_{dAu}$  for pions and protons in two momentum bins. The modification factors are plotted as a function of  $\nu = N_{coll}/N_{part}^d$ , the number of collisions per participating deuteron nucleon. The lower momentum bin, for  $0.6 \leq p_T \leq 1.0$  GeV/c, is chosen in the region where  $R_{dAu}$  is less than 1.0, and hadron yields scale very nearly with the number of nucleons participating in the collision, rather than with the number of binary collisions. As expected,  $R_{dAu}$  decreases with  $\nu$  in this  $p_T$  range, with negligible difference between pions and protons. In the higher  $p_T$  bin,  $R_{dAu}$  increases with the number of collisions, with a notably larger rate of increase for baryons

than for mesons. Though the  $R_{dAu}$  values for higher  $p_T$  hadrons appear to flatten with increasing centrality, the uncertainties are too large to allow a definitive conclusion about saturation with the number of collisions suffered by each participant nucleon [14].

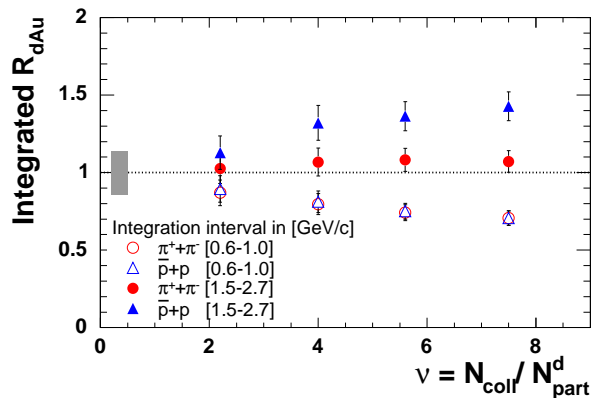


FIG. 12: (color online) Integrated  $R_{dA}$  for pions and protons in two momentum bins as a function of the number of collisions suffered by the deuteron participant  $\nu$ . Error bars indicate the quadrature sum of statistical errors and uncertainties on the number of collisions bin-by-bin. The solid box on the left shows the magnitude of the centrality independent uncertainties.

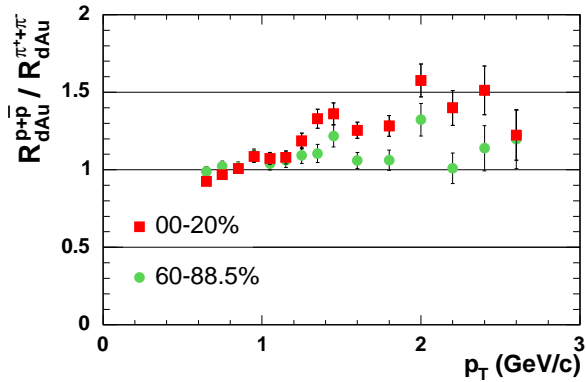


FIG. 13: (color online) Ratio of the proton over the pion nuclear modification in d+Au collisions, for central and peripheral events. Error bars indicate statistical errors only.

#### D. Cronin Effect For Baryons

Figure 13 shows the ratio of the nuclear modification factors observed for protons and antiprotons to that for pions in the most central and the most peripheral d+Au collisions. The enhancement for protons is stronger, by approximately 30%-50% in the most central collisions; this was also reported by STAR [34]. The increasing difference between baryons and mesons for more central collisions indicates that the baryon production mechanism appears to depend upon the surrounding nuclear medium already in d+Au collisions. We note, however, that the species dependence of the Cronin effect in d+Au collisions is much smaller than the factor of  $\approx 3$  enhancement of protons in central Au+Au collisions, as can be seen by comparing the nuclear modification factors for pions and protons in central Au+Au collisions shown below in section IV A.

By converting the nuclear modification factors to per-beam-nucleon cross section ratios and vice versa, it is possible to compare to measurements of the Cronin effect at other energies. Figure 14 shows nuclear modification factors from this work compared to those derived from  $\alpha$ -factors measured at lower energies [2], in a similar manner to that used in [3] to calculate per-nucleon cross section ratios. In order to make the transition to nuclear modification factors from per-nucleon cross section ratios we assume that  $\sigma_{d+A} = 2 \times \sigma_{p+A}$  and  $\sigma_{p+d} = 2 \times \sigma_{p+p}$  at the low energy of interest, which is a very reasonable approximation for all particle species [2].

The observed species dependence of the enhancement is similar to that measured in lower energy collisions [3]. The magnitude of the enhancement for pions at  $p_T > 3$  GeV/c is larger at  $\sqrt{s} = 27.4$  GeV than at 200 GeV. Protons and antiprotons are also more enhanced at the lower beam energy: a factor of 3.5 at  $p_T \approx 4$  GeV, as compared with a factor of 2 at  $\sqrt{s} = 200$  GeV. This energy dependence of the Cronin effect for pions has been interpreted

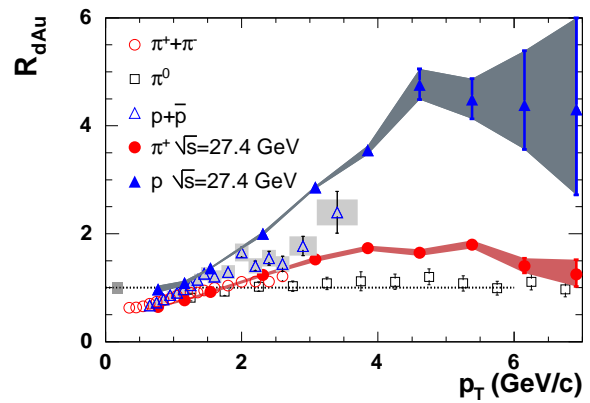


FIG. 14: Nuclear modification factors for charged pions, neutral pions [33], and protons and antiprotons from minimum bias d+Au from this work (shown by open symbols) compared to nuclear modification factors calculated from the per-beam nucleon cross sections reported for  $\sqrt{s} = 27.4$  GeV p + A collisions [2] (closed symbols and continuous bands)

as evidence for a different production mechanism for high  $p_T$  hadrons at RHIC compared to lower energies [35]. In this model, high  $p_T$  hadrons are produced incoherently on different nucleons at low energy, while in higher energy collisions the production amplitudes can interfere because the process of gluon radiation is long compared to the binary collision time. Coherent radiation from different nucleons is subject to Landau-Pomeranchuk suppression. However, the difference between baryon and meson Cronin effect is not predicted by this model.

## IV. DISCUSSION

Traditional explanations of the Cronin effect all involve multiple scattering of incoming partons that lead to an enhancement at intermediate  $p_T$  [12]. There are various theoretical models of the multiple scattering, which predict somewhat different dependence upon the number of scattering centers. The observed centrality or  $\nu$  dependence for pions is well-reproduced by semi-hard initial state scattering [13] as shown in Fig. 11; see also [14, 15, 16]. The models include initial state multiple scattering as well as geometrical shadowing. However, none of these models would predict a species dependent Cronin effect, as initial state parton scattering precedes fragmentation into the different hadronic species. The markedly larger Cronin effect for protons and antiprotons requires processes in addition to initial state multiple scattering in baryon production at moderate transverse momenta.

Recently, Hwa and collaborators [17] have shown an alternative explanation of the Cronin effect, attributed to the recombination of shower quarks with those from

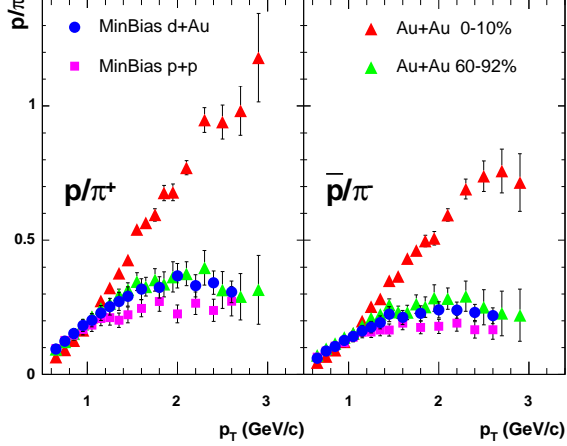


FIG. 15: (color online) The ratio of feed-down corrected protons to  $\pi^+$  and antiprotons to  $\pi^-$  in minimum bias p+p and d+Au compared to peripheral and central Au+Au collisions. Statistical error bars are shown.

the medium in d+Au collisions. Such models do predict a larger Cronin effect for protons than pions, and may be justified by the rather short formation times of  $p_T = 2 - 4$  GeV/c protons. According to the uncertainty principle, the formation time in the rest frame of the hadron can be related to the hadron size  $R_h$ . In the laboratory frame, the formation time of a hadron with mass  $m_h$  and energy  $E_h$  is given by  $\tau_f \approx R_h \frac{E_h}{m_h}$ . For a  $p_T = 2.5$  GeV/c pion, the formation time is 9-18 fm/c (for  $R_h = 0.5 - 1.0$  fm), well outside the collision region. However, for  $p_T = 2.5$  GeV/c protons, the corresponding formation time is only 2.7 fm/c, suggesting that the hadronization process may well begin in or near the nuclear medium.

### A. Comparison to Au+Au Collisions

The proton to pion ratio from minimum bias p+p and minimum bias d+Au are compared to each other and to central and peripheral Au+Au collisions in Fig. 15. As noted above, protons and antiprotons are feed-down corrected in each system.

The  $p/\pi$  ratio in d+Au is very similar to that in peripheral Au+Au collisions, and lies slightly above the p+p ratio. The  $p/\pi$  ratio in central Au+Au collisions is, however, much larger. The difference between the ratio in d+Au and central Au+Au clearly indicates that baryon yield enhancement is not simply an effect of sampling a large nucleus in the initial state. The large enhancement requires the presence of a substantial volume of nuclear medium.

Figures 16, 17 and 18 compare the nuclear modification factors for pions, kaons and (anti)protons in Au+Au and d+Au collisions. The p+p data from this work allow,

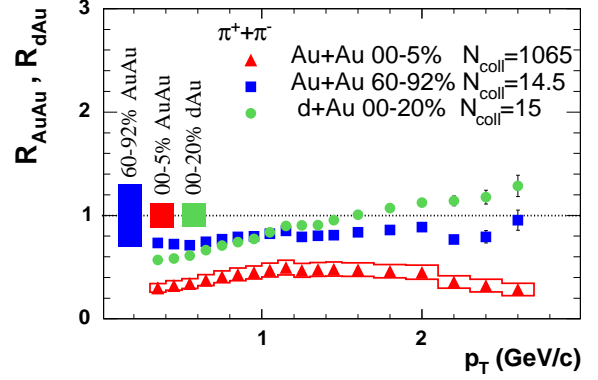


FIG. 16: (color online) Nuclear modification factors for pions, comparing central and peripheral Au+Au collisions to central d+Au. It should be noted that the number of binary nucleon-nucleon collisions in peripheral Au+Au and central d+Au is very similar. Solid bars on the left indicate normalization uncertainties in the p+p absolute cross section and in the calculation of  $N_{coll}$  for the three systems. Error bars indicate statistical errors only, while for the most central Au+Au case the systematic errors, discussed in the text, are shown as boxes around the points.

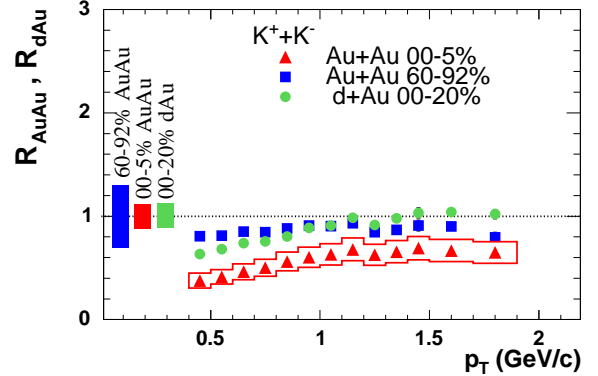


FIG. 17: (color online) Nuclear modification factors for kaons, comparing central and peripheral Au+Au collisions to central d+Au. Statistical and systematic errors are represented as in Fig. 16.

for the first time, the calculation of nuclear modification factors in Au+Au by PHENIX. The Au+Au data are taken from reference [7]. It should be noted that common fluctuations between  $R_{dAu}$  and  $R_{AuAu}$  in Figures 17 and 18 arise because the p+p denominators are common.

Central and peripheral Au+Au collisions are compared to central d+Au collisions, which have a similar number of binary collisions as the peripheral Au+Au sample. Pions show a much lower  $R_{AA}$  at high  $p_T$  in central than in peripheral Au+Au collisions, as expected from the large energy loss suffered by the partons in central collisions.

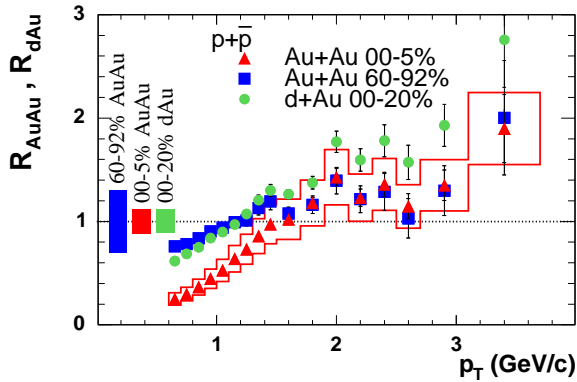


FIG. 18: (color online) Nuclear modification factors for protons and antiprotons, comparing central and peripheral Au+Au collisions to central d+Au. Statistical and systematic errors are represented as in Fig. 16.

The nuclear modification factor rises faster with  $p_T$  in d+Au than in peripheral Au+Au, despite the comparable number of binary collisions. As Au+Au involves a second Au nucleus, shadowing effects can be expected to be larger, reducing the observed Cronin effect.

The proton and antiproton nuclear modification factors show a quite different trend. The Cronin effect, larger than 1.0 at higher  $p_T$  values, is independent of centrality in Au+Au collisions. This feature was already observed as binary collision scaling of proton and antiproton production in the central/peripheral collision yield ratios [6]. The Cronin effect in d+Au is at least as large as in peripheral Au+Au. The difference indicates that baryon production must involve a complex interplay of processes in addition to initial state nucleon-nucleon collisions.

## V. CONCLUSION

We have presented the centrality and species dependence of identified particle spectra in d+Au collisions, including the dependence of the nuclear modification factor upon the number of collisions per participant nucleon. We also presented the first measurement of  $R_{AA}$  for pions, kaons, protons and antiprotons in Au+Au collisions.

The Cronin effect for charged pions is small, but non-zero. The proton to pion ratio in d+Au is similar to that in peripheral Au+Au, while the corresponding ratio in p+p is somewhat lower. The nuclear modifica-

tion factor in d+Au for protons shows a larger Cronin effect than that for pions, and the difference increases with collision centrality. This difference was seen, but never fully understood, in lower energy collisions, and is not large enough to account for the abundance of protons in central Au+Au collisions. The difference between pions and protons does, however, indicate that the Cronin effect is not simply due to multiple scattering of the incoming partons.  $R_{AA}$  for protons and antiprotons confirms previous observations that the production of high  $p_T$  baryons in Au+Au scales with the number of binary nucleon-nucleon collisions, but the baryon yield per collision in Au+Au exceeds that in p+p.

## Acknowledgements

We thank the staff of the Collider-Accelerator and Physics Departments at Brookhaven National Laboratory and the staff of the other PHENIX participating institutions for their vital contributions. We acknowledge support from the Department of Energy, Office of Science, Office of Nuclear Physics, the National Science Foundation, Abilene Christian University Research Council, Research Foundation of SUNY, and Dean of the College of Arts and Sciences, Vanderbilt University (U.S.A), Ministry of Education, Culture, Sports, Science, and Technology and the Japan Society for the Promotion of Science (Japan), Conselho Nacional de Desenvolvimento Científico e Tecnológico and Fundação de Amparo à Pesquisa do Estado de São Paulo (Brazil), Natural Science Foundation of China (People's Republic of China), Centre National de la Recherche Scientifique, Commissariat à l'Énergie Atomique, and Institut National de Physique Nucléaire et de Physique des Particules (France), Ministry of Industry, Science and Technologies, Bundesministerium für Bildung und Forschung, Deutscher Akademischer Austausch Dienst, and Alexander von Humboldt Stiftung (Germany), Hungarian National Science Fund, OTKA (Hungary), Department of Atomic Energy (India), Israel Science Foundation (Israel), Korea Research Foundation, Center for High Energy Physics, and Korea Science and Engineering Foundation (Korea), Ministry of Education and Science, Russia Academy of Sciences, Federal Agency of Atomic Energy (Russia), VR and the Wallenberg Foundation (Sweden), the U.S. Civilian Research and Development Foundation for the Independent States of the Former Soviet Union, the US-Hungarian NSF-OTKA-MTA, and the US-Israel Binational Science Foundation.

[1] J.W. Cronin *et al.*, Phys. Rev. D **11**, 3105 (1975).  
 [2] D. Antreasyan *et al.*, Phys. Rev. D **19**, 764 (1979).  
 [3] P.B. Straub *et al.*, Phys. Rev. Lett. **68**, 452 (1992).

[4] K. Adcox *et al.*, [PHENIX Collaboration], Phys. Rev. Lett. **88**, 022301 (2002).  
 [5] K. Adcox *et al.*, [PHENIX Collaboration], Phys. Rev.

- Lett. **88**, 242301 (2002).
- [6] S.S. Adler *et al.* [PHENIX Collaboration], Phys. Rev. Lett. **91**, 172301 (2003).
- [7] S.S. Adler *et al.*, [PHENIX Collaboration]. Phys. Rev. **C69**, 034909 (2004).
- [8] B. Alper *et al.*, Nucl. Phys. **B100**, 237 (1975).
- [9] R.C. Hwa and C.B. Yang, Phys. Rev. **C67**, 034902 (2003) and Phys. Rev. **C70**, 037901 (2003); R.J. Fries, B. Muller, C. Nonaka and S.A. Bass Phys. Rev. Lett. **90**, 202303 (2003) and Phys. Rev. **C68**, 044902 (2003); V. Greco, C.M. Ko and P. Levai, Phys. Rev. Lett. **90**, 202302 (2003) and Phys. Rev. **C68**, 034904 (2003).
- [10] G. Rossi and G. Veneziano, Nucl. Phys. **B123**, 507 (1977); D. Kharzeev, Phys. Lett. **B378**, 238 (1996); S.E. Vance, M. Gyulassy and X.-N. Wang, Phys. Lett. **B443**, 45 (1998).
- [11] D. Kharzeev, E. Levin and L. McLerran, Phys. Lett. **B561**, 93 (2003).
- [12] M. Lev and B. Petersson, Z. Phys. **C21**, 155 (1983).
- [13] A. Accardi and M. Gyulassy, Phys. Lett. **B586**, 244 (2004).
- [14] G. Papp, P. Levai, G. Fai, Phys. Rev. **C61**, 021902(R) (1999).
- [15] I. Vitev, M. Gyulassy, Phys. Rev. Lett. **89**, 252301 (2002).
- [16] X.N. Wang, Phys. Rev. **C61**, 064910 (2000).
- [17] R.C. Hwa and C.B. Yang, Phys. Rev. Lett. **93**, 082302 (2004).
- [18] K. Adcox *et al.*, [PHENIX Collaboration], Nucl. Instrum. Methods **A499**, 469 (2003). In addition to this overview, detailed descriptions of individual subsystems are published in the same volume.
- [19] K.A. Drees and Z. Xu, "Proceedings of the PAC2001 Conference" 3120 (2001). <http://epaper.kek.jp/p03/PAPERS/TPPB032.PDF>
- [20] R. Brun, R. Hagelberg, N. Hansroul and J. Lassalle, CERN-DD-78-2 (1978).
- [21] S.S. Adler *et al.*, [PHENIX Collaboration], Phys. Rev. Lett. **96**, 012304 (2006).
- [22] R.J. Glauber and G. Matthiae, Nucl. Phys. **B21**, 135 (1970).
- [23] S.S. Adler *et al.* [PHENIX Collaboration], Phys. Rev. Lett. **94**, 082302 (2005).
- [24] L. Hulthén and M. Sagawara, Handbuch der Physik **39** (1957).
- [25] K. Adcox *et al.*, [PHENIX Collaboration], Nucl. Instrum. Methods **A482**, 491 (2002).
- [26] R.E. Ansorge *et al.*, [UA5 Collaboration], Nucl. Phys. **B328**, 36 (1989).
- [27] J. Adams and M. Heinz, [STAR Collaboration], nucl-ex/0403020, (2004).
- [28] M. Heinz, [STAR Collaboration], J. Phys. G **31**, S141 (2005).
- [29] X. Z. Cai, [STAR Collaboration], J. Phys. G **31**, S1015 (2005).
- [30] R. Witt, [STAR Collaboration], nucl-ex/0403021 (2004).
- [31] B.B. Back *et al.*, [PHOBOS Collaboration], Phys. Rev. **C70**, 011901 (2004); Phys. Rev. **C71**, 021901 (2005).
- [32] I.G. Bearden *et al.*, [BRAHMS Collaboration], Phys. Lett. **B607**, 42 (2005).
- [33] S.S. Adler *et al.*, [PHENIX Collaboration], Phys. Rev. Lett. **91**, 072303 (2003).
- [34] J. Adams *et al.*, [STAR Collaboration], Phys. Lett. **B616**, 8 (2005).
- [35] B.Z. Kopeliovich, J. Nemchik, A. Schafer and A.V. Tarasov, Phys. Rev. Lett. **88**, 232303 (2002).